Enhanced photocatalytic performance of porous MoS_2 structures for methyl orange degradation in simulated sunlight

Ly Manh Quan[1, 2], Tran Dinh Thinh[3], Nguyen Van Khanh[1], Tran Quynh Chi[1], La Duc Duong[3], Nguyen Minh Phuong[1*]

[1]Faculty of Environmental Sciences, VNU University of Science, 334 Nguyen Trai, Thanh Xuan, Hanoi, Vietnam;
[2]Military Institute of Environmental Chemistry, An Khanh, Hanoi, Vietnam;
[3]Institute of Materials, Biology and Environment, 17 Hoang Sam, Nghia Do, Hanoi, Vietnam.
[*]Corresponding author: nguyenminhphuong@hus.edu.vn
Received 15 Aug. 2025; Revised 30 Sep. 2025; Accepted 16 Oct. 2025; Published 18 Nov. 2025.
DOI: https://doi.org/10.54939/1859-1043.j.mst.IMBE.2025.88-94

ABSTRACT

In this study, porous MoS_2 nanoflowers (NFs) were synthesized using a simple hydrothermal method and tested for their photocatalytic efficiency in degrading methyl orange (MO) under simulated sunlight. The MoS_2 NFs possess a hierarchical structure formed by ultrathin nanosheets, which provide a large surface area and active edge sites, enhancing light absorption and facilitating efficient charge separation. Photocatalytic experiments demonstrated an impressive degradation efficiency of more than 60% for MO dyes after 120 minutes of reaction with a degrading rate of 2.51 x 10^{-2} min^{-1}. The enhanced photocatalytic performance is attributed to the high crystallinity, a large surface-to-volume ratio, and efficient charge carrier dynamics provided by the porous MoS_2 nanoflower structure. These findings suggest that MoS_2 nanostructures are highly promising as efficient and stable photocatalysts for practical applications in wastewater treatment under solar irradiation, offering potential for sustainable environmental remediation.

Keywords: MoS_2 nanoflowers; Photocatalysis; Methylene orange; Reactive oxygen species; Solar irradiation.

1. INTRODUCTION

The increasing discharge of synthetic dyes into water bodies, particularly from textile and printing industries, poses a serious environmental threat due to their toxicity, persistence, and resistance to natural degradation [1, 2]. Among these, methyl orange (MO) is widely used as a model pollutant in photocatalytic studies because of its structural stability and high solubility in water [3].

Conventional wastewater treatment methods are often ineffective in removing persistent organic pollutants such as methyl orange (MO), especially at trace concentrations [4]. Among emerging technologies, advanced oxidation processes (AOPs), particularly photocatalysis, have garnered significant attention due to their ability to generate highly oxidative hydroxyl radical (˙OH), enabling the effective degradation of persistent organic pollutants without producing secondary contaminants [5].

Photocatalytic degradation using semiconductor materials has attracted widespread attention as a green and effective approach for treating dye-containing wastewater. Molybdenum disulfide (MoS_2), a transition metal dichalcogenide (TMD) with a layered structure, has gained significant attention as a multifunctional material for photocatalytic applications due to its moderate bandgap (1.2–1.9 eV), high surface-to-volume ratio, tunable electronic structure, and chemical stability [6, 7].

Recent studies have shown that the photocatalytic performance and HER of MoS_2 can be significantly improved by engineering its morphology into hierarchical nanostructures, such as nanospheres, nanosheets, and nanoflowers [8, 9]. Among these, flower-like MoS_2 structures are particularly attractive because they offer a large specific surface area and abundant edge sites,

facilitating light absorption and charge separation [10]. Specifically, three-dimensional (3D) nanostructures, such as flower-like and ultrathin nanosheet assemblies, provide enhanced performance by offering a larger number of exposed edge sites, improved light-harvesting ability, and more efficient separation of photoinduced electron–hole pairs [11]. For instance, Xian Yan et al. [6] reported that the integration of 3D MoS_x nanoflowers with CoP nanoparticles significantly improved HER performance by generating dual proton-adsorption sites. Similarly, Ya Yan et al. [7] demonstrated that ultrathin MoS_2 nanosheets with high edge density were better at photocatalytic activity than bulk MoS_2 due to their expanded surface area and higher density of unsaturated sites.

Among various synthesis methods, the hydrothermal approach stands out for its ability to produce MoS_2 nanostructures with high crystallinity and uniform morphology under mild reaction conditions, while offering scalability and cost-effectiveness. Solution-based synthesis enables precise control over the morphology and size of nanostructures, such as nanowires, nanotubes, and nanosheets, through a simple and reproducible process, making it suitable for fabricating high-purity nanocrystals [12].

Several studies have reported the photocatalytic degradation of methyl orange (MO) using MoS_2 synthesized by different approaches. For instance, Yang et al. (2022) achieved up to 93.8% removal of MO within 60 min using hydrothermally prepared MoS_2 nanoflowers [17]. Tien et al. (2022) developed MoS_2/Co_3O_4 nanohybrids that degraded 95.6% of MO in 170 min with good recyclability [18].

In this study, porous MoS_2 nanoflowers were synthesized via a hydrothermal route and their photocatalytic performance in degrading methyl orange under simulated sunlight was evaluated. The effects of synthesis conditions on the morphology and photocatalytic activity of the materials were systematically investigated, with the aim of developing an efficient, low-cost photocatalyst for wastewater treatment.

2. EXPERIMENTAL METHODS

2.1. Materials

Ammonium molybdate tetrahydrate $(NH_4)_6Mo_7O_{24}\cdot 4H_2O$ (99%) was supplied from Tianjin Kaihua Chemical Reagent Factory (China), Thiourea CH_4N_2S (99%) was purchased from Xilong Scientific (China), Centyl trimethylammonium Bromide CTAB (99%) was obtained from Adamas-beta (China), Methyl Orange (MO).

2.2. Synthesis of MoS_2 nanoflowers

MoS_2 nanoflowers were prepared via the hydrothermal method. $(NH_4)_6Mo_7O_{24}.4H_2O$ (0,617 g), CH_4N_2S (0,76 g) and CTAB were dissolved in 40 mL deionized water. The mixture was magnetically stirred for 15 minutes and then subjected to hydrothermal treatment at 200 ^oC for 24 hours using a Memmert furnace (Germany). The obtained precipitated product was collected by centrifugation at 4000 rpm for 5 minutes and washed several times with distilled water and ethanol to remove residual solvent and impurities on the surface. The product was subsequently dried at 80 °C overnight, followed by annealing under an inert nitrogen atmosphere at 350 °C for 3 hours, with a heating rate of 2 °C min^{-1} [19].

2.3. Material characterizations

The morphological, compositional, and optical properties of the flower-like MoS_2 nanostructures were characterized using various advanced techniques. Field-emission scanning electron microscopy (FE-SEM, JEOL JSM-7600F) and high-resolution transmission electron microscopy (HRTEM, JEOL 2100F) methods were applied to reveal the surface morphological characteristics of the as-prepared material. The EDS (Energy-dispersive X-ray spectroscopy, Bruker D8 Advance, Cu-$K_{\alpha 1}$, λ = 1.54056 Å) analysis confirmed the elemental compositions.

Raman (Renishaw InVia confocal micro-Raman) and Photoluminescence (PL, iHR550, Horiba, λ = 325 nm) spectroscopy were employed to investigate the vibrational features and photoluminescence behavior of the material.

2.4. Photocatalytic experiments

The photocatalytic performance was evaluated via the time-dependent degradation efficiency of methyl orange (MO), photodegradation kinetics, and kinetic studies under simulated sunlight irradiation for 120 minutes.

The degradation kinetics of MO were investigated using a pseudo-first-order model based on the Langmuir–Hinshelwood mechanism, which is commonly applied to heterogeneous photocatalysis. The linearized form of the kinetic equation is:

$$-\ln(C_t/C_0) = k.t \quad (1)$$

Where: k is the apparent rate constant (min^{-1});

t is the irradiation time (min);

C_0 and Ct are the dye concentrations at time 0 and *t*, respectively.

3. RESULTS AND DISCUSSION

3.1. Morphological and microstructural characterization

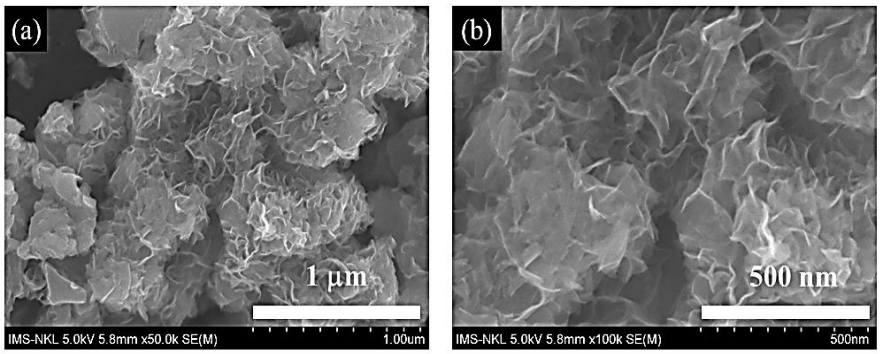

Figure 1. *SEM images of MoS_2 nanoflowers obtained after annealing at 350 °C under a Nitrogen atmosphere.*

Figure 1 presents SEM images of the synthesized MoS_2 material at two magnifications. At ×50,000 magnification (figure 1a), the material exhibits a distinctive nanoflower-like morphology, consisting of multiple thin nanosheets stacked and interconnected into a three-dimensional hierarchical structure. The average diameter of the nanoflower assemblies is approximately 500 - 800 nm.

At ×100,000 magnification (figure 1b), the nanosheets forming the "petals" display wrinkled surfaces and a loosely stacked arrangement - typical features of two-dimensional layered MoS_2.

This hierarchical morphology not only provides a large specific surface area and a high density of active edge sites but also enhances light-harvesting capability and facilitates mass transport. Furthermore, the multi-tiered porous architecture can improve the separation and transport efficiency of photogenerated electron–hole pairs under illumination, thereby significantly promoting the photocatalytic performance of the material.

Figures 2a and 2b (low-magnification TEM images) reveal that the MoS_2 nanosheets are ultrathin, wrinkled, and loosely stacked, forming a nanoflower morphology consistent with the SEM observations. The lateral dimensions of these nanosheets range from several tens to several hundreds of nanometers, and the contrast variation indicates their few-layered nature. The high-resolution TEM (HRTEM) image in figure 2c distinctly displays the stacked-layer arrangement of

MoS_2 nanosheets, with interlayer spacings clearly visible at the sheet edges. This spacing matches well with the characteristic value of the 2H-phase MoS_2. In figure 2d, well-resolved lattice fringes are observed with an interplanar spacing of approximately 0.62 nm, corresponding to the (002) crystal plane of hexagonal MoS_2. The results confirm the high crystallinity and the well-preserved layered structure of the material.

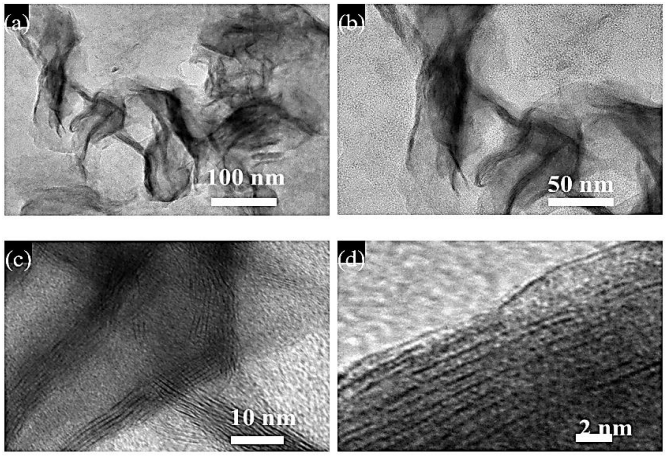

Figure 2. *TEM images of MoS_2 nanoflowers obtained after annealing at 350 °C under nitrogen.*

Such morphological and structural characteristics are expected to enhance photocatalytic activity by providing a large specific surface area, abundant active edge sites, and efficient charge transport channels.

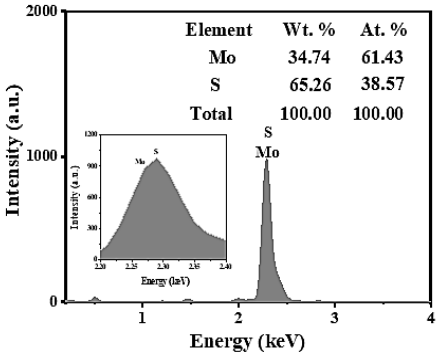

Figure 3. *EDS spectrum of MoS_2 nanoflowers obtained after annealing at 350 °C under a nitrogen atmosphere.*

Figure 3 shows the EDS spectrum of the synthesized MoS_2 nanoflowers, confirming their elemental composition. Two distinct peaks are observed, corresponding to molybdenum (Mo) and sulfur (S) - the primary constituents of MoS_2. The strong peak at approximately 2.3 keV is attributed to sulfur, while the adjacent peak at slightly lower energy corresponds to molybdenum. No significant signals from other elements are detected, indicating the high purity of the synthesized product. Quantitative analysis reveals weight percentages of 34.74% for Mo and 65.26% for S, with corresponding atomic percentages of 61.43% for Mo and 38.57% for S. Overall, the EDS results confirm the successful synthesis of high-purity MoS_2 with good elemental stoichiometry and negligible contamination.

Figure 4 illustrates the Raman spectrum (figure 4a) and photoluminescence (PL) spectrum (figure 4b) of the MoS_2 nanoflowers. In the Raman spectrum, two prominent peaks are observed at approximately 382 cm^{-1} and 407 cm^{-1}, corresponding to the in-plane E_2g^1 and out-of-plane A_1g

vibrational modes of the 2H-phase MoS_2, respectively. The frequency difference of ~25 cm^{-1} between these peaks is indicative of few-layer MoS_2. The sharp and intense peaks confirm the high crystallinity of the nanostructures. In figure 4.b, the PL spectrum exhibits two broad emission bands centered at 503 nm and 715 nm. The 503 nm emission is attributed to the direct bandgap transition in few-layer MoS_2, while the 715 nm peak is likely related to defect-mediated recombination and trap states within the band structure. The overall low PL intensity suggests efficient separation of photogenerated electron - hole pairs - an advantageous feature for photocatalytic applications.

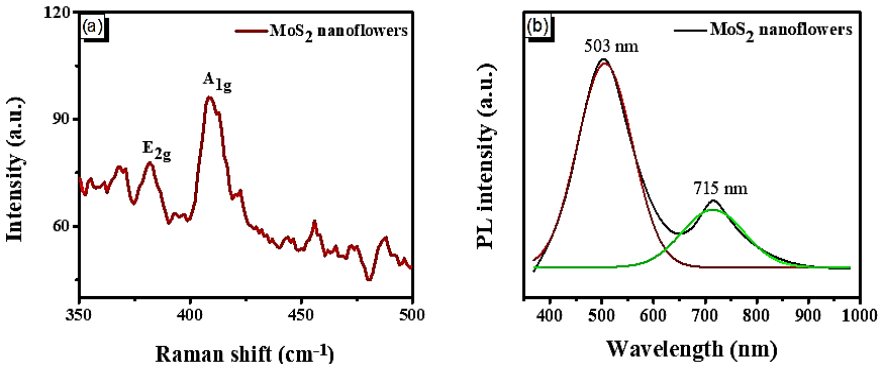

Figure 4. *Raman and PL spectra of MoS_2 nanoflowers obtained after annealing at 350 °C under a nitrogen atmosphere.*

3.2. Photodegradation activity

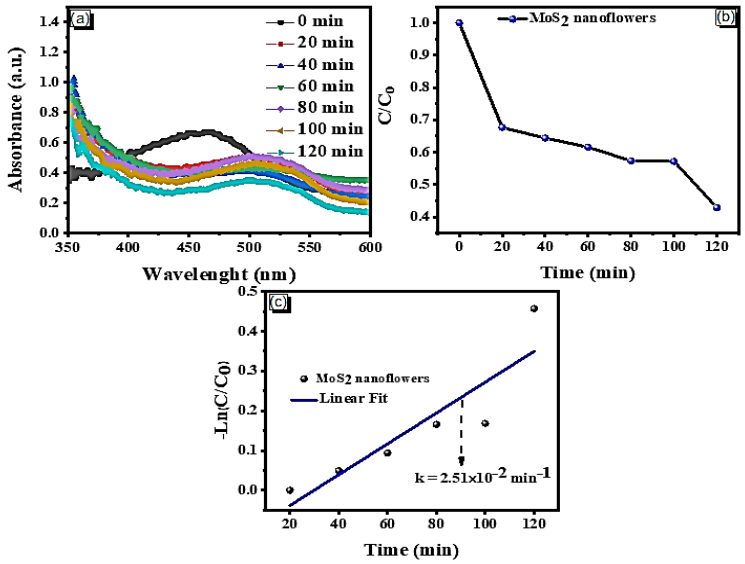

Figure 5. *(a) Time-dependent photocatalytic degradation efficiency of MO using porous MoS_2 nanoflowers, (b) photodegradation kinetics, and (c) kinetic study under simulated sunlight irradiation over 120 min.*

The photocatalytic performance was evaluated based on the degradation of MO under visible-light irradiation. In this study, the initial concentration of MO was 0.02 ppm. All experiments were conducted under magnetic stirring at a temperature of 20 – 25 °C, and pH was maintained between 5.0 – 6.0 to ensure stable reaction conditions. The characteristic absorption peak of MO at ~ 465 nm gradually decreased with increasing irradiation time (figure 5a), indicating the cleavage of azo (-N=N-) bonds, which are responsible for the color and structural stability of the dye molecules [13].

The C/C_0 versus time plot (figure 5b) shows that the C/Co value decreased from 1.0 to approximately 0.43 after 120 minutes of irradiation, corresponding to a degradation efficiency of about 57%.

As described in Eq.01, the plot of $-\ln(C_t/C_0)$ versus time (figure 5c) yields a straight line, with the slope representing the rate constant k.

In this study, the calculated value of k is:

$$k = 2.51 \times 10^{-2} \text{ min}^{-1}$$

This relatively high rate constant indicates higher photocatalytic efficiency compared to previously reported MoS_2-based catalysts [14, 15].

The enhanced activity is attributed to multiple synergistic factors, including:

(i) efficient light harvesting by the layered MoS_2,

(ii) effective charge separation enabled by the thin nanosheet structure,

(iii) a large number of exposed active edge sites,

(iv) possible generation of reactive oxygen species (ROS) such as •OH and $\bullet O_2^-$ during the photocatalytic process [16].

4. CONCLUSIONS

In this study, porous MoS_2 nanoflowers were successfully synthesized via a simple hydrothermal method and evaluated for photocatalytic degradation of methyl orange (MO) under simulated sunlight irradiation. Morphological and structural analyses revealed that the material consists of ultrathin nanosheets assembled into a three-dimensional hierarchical architecture, offering a large specific surface area, abundant active edge sites, and strong light absorption capability. Raman, PL, and EDS analyses confirmed the high crystallinity, few-layer structure, and high purity of the synthesized MoS_2, while TEM/HRTEM observations verified the interlayer spacing consistent with the 2H-MoS_2 phase. These structural features contributed to improved charge separation and transport, effectively suppressing electron–hole recombination. Photocatalytic tests demonstrated that the porous MoS_2 nanoflowers achieved a degradation efficiency of ~57% for MO after 120 minutes, with a rate constant of 2.51×10^{-2} min^{-1} - superior to many MoS_2-based photocatalysts reported in the literature. This enhanced performance is attributed to the synergistic effects of efficient light harvesting, ultrathin nanosheet morphology, high density of active edge sites, and the generation of reactive oxygen species (ROS) during the photocatalytic process.

REFERENCES

[1]. Forgacs, E., Cserháti, T., Oros, G., *"Removal of synthetic dyes from wastewaters: a review"*, Environmental International, 30(7), 953–971 (2004).

[2]. Robinson, T. et al., *"Remediation of dyes in textile effluent: a critical review on current treatment technologies with a proposed alternative"*, Bioresource Technology, 77(3), 247–255 (2001).

[3]. Fujishima, A., Honda, K., *"Electrochemical photolysis of water at a semiconductor electrode"*, Nature, 238, 37–38 (1972).

[4]. Ahmed, M. A., Mahmoud, S. A., Mohamed, A. A., *"Interfacially engineered metal oxide nanocomposites for enhanced photocatalytic degradation of pollutants and energy applications"*, RSC Advances. DOI: https://doi.org/10.1039/D4RA08780A

[5]. Sivaranjani, P. R., Janani, B., Thomas, A. M., Raju, L. L., Khan, S. S., *"Recent development in MoS2-based nano-photocatalyst for the degradation of pharmaceutically active compounds"*, Journal of Cleaner Production, 352, 131506 (2022). DOI: https://doi.org/10.1016/j.jclepro.2022.131506

[6]. Yan, X. et al., *"3D layered nano-flower MoSx anchored with CoP nanoparticles form double proton adsorption site for enhanced photocatalytic hydrogen evolution under visible light driven"*, International Journal of Hydrogen Energy, 45, 2578–2592 (2020).

[7]. Yan, Y., Xia, B., Ge, X., Liu, Z., Wang, J.-Y., Wang, X., *"Ultrathin MoS2 Nanoplates with Rich Active Sites as Highly Efficient Catalyst for Hydrogen Evolution"*, ACS Applied Materials & Interfaces, 5, 12794–12798 (2013). DOI: https://doi.org/10.1021/am404843b

[8]. Wang, Q. H., Kalantar-Zadeh, K., Kis, A., Coleman, J. N., Strano, M. S., *"Electronics and optoelectronics of two-dimensional transition metal dichalcogenides"*, Nature Nanotechnology, 7, 699–712 (2012).

[9]. Sun, Y., Zhang, Y., Zheng, S., Wang, C., *"Facile synthesis of flower-like MoS_2 nanostructures and their application in photocatalytic degradation of methylene blue"*, Journal of Materials Science, 51, 10362–10371 (2016).

[10]. Yu, X., Zhang, H., Cui, H., Yang, Y., *"Hydrothermal synthesis of porous MoS_2 nanoflowers for enhanced visible-light photocatalytic activity"*, Materials Letters, 142, 276–279 (2015).

[11]. Xiao, X., Wang, Y., Cui, B., Zhang, X., Zhang, D., Xu, X., *"Preparation of MoS2 nanoflowers with rich active sites as an efficient adsorbent for aqueous organic dyes"*, New Journal of Chemistry, (n.d.). DOI: https://doi.org/10.1039/D0NJ00129E

[12]. Ghamarpoor, R., Fallah, A., Jamshidi, M., *"A Review of Synthesis Methods, Modifications, and Mechanisms of ZnO/TiO2-Based Photocatalysts for Photodegradation of Contaminants"*, ACS Omega, 9, 25457–25492 (2024). DOI: https://doi.org/10.1021/acsomega.3c08717

[13]. Zhang, X., et al., *"Photocatalytic degradation of methyl orange by MoS_2 nanosheets under visible light irradiation"*, Applied Catalysis B: Environmental, 147, 229–235 (2014). DOI: https://doi.org/10.1016/j.apcatb.2013.09.031

[14]. Zhang, H., et al., *"Visible-light-driven photocatalytic degradation of organic pollutants by few-layer MoS_2 nanosheets"*, Nanotechnology, 24(28), 285706 (2013).

[15]. Liu, S., et al., *"Morphology-dependent photocatalytic activity of MoS_2 nanostructures"*, Materials Letters, 276, 128192 (2020).

[16]. Wang, C., et al., *"Charge separation in 2D MoS_2-based composites for photocatalysis"*, Chemical Engineering Journal, 420, 129702 (2021).

[17]. Yang, X., Wen, L., et al., *"Hydrothermal synthesis of MoS2 nanoflowers and its rapid adsorption of tetracycline"*, Solid State Sciences, 133, 107014 (2022).

[18]. Tien, T.-M., Chao-Hsiang, et al., *"Photocatalytic Degradation of Methyl Orange Dyes Using Green Synthesized MoS2/Co3O4 Nanohybrids"*, Catalysts, 12(11), 1474 (2022). DOI: https://doi.org/10.3390/catal12111474

[19]. Zhang, H., Cong, L., et al., *"Impact of CTAB on morphology and electrochemical performance of MoS2 nanoflowers with improved lithium storage properties"*, Journal of Materials Science: Materials in Electronics, 29, 3631–3639 (2018). DOI: https://doi.org/10.1007/s10854-017-8293-4

TÓM TẮT

Hoạt tính quang xúc tác phân hủy methyl orange của vật liệu cấu trúc xốp MoS_2 dưới chiếu xạ ánh sáng mặt trời mô phỏng

Trong nghiên cứu này, vật liệu MoS_2 dạng cấu trúc "hoa nano" xốp (NFs) đã được tổng hợp bằng phương pháp thủy nhiệt đơn giản và khảo sát hoạt tính quang xúc tác phân hủy phẩm nhuộm Methyl Orange (MO) dưới ánh sáng mặt trời mô phỏng. Cấu trúc MoS_2 NFs được hình thành từ các nanosheet siêu mỏng, cung cấp diện tích bề mặt lớn và nhiều vị trí hoạt tính, giúp tăng cường khả năng hấp thụ ánh sáng và thúc đẩy tách tải điện hiệu quả. Thí nghiệm quang xúc tác cho thấy hiệu suất phân hủy MO vượt 60% sau 120 phút phản ứng, với hằng số tốc độ phân hủy đạt $2{,}51 \times 10^{-2}$ phút^{-1}. Hiệu quả phân hủy MO của vật liệu được lý giải bởi độ kết tinh cao, tỷ lệ bề mặt/thể tích lớn và động học truyền tải điện tích tối ưu của cấu trúc hoa nano xốp. Những kết quả này cho thấy các cấu trúc nano MoS_2 là vật liệu quang xúc tác tiềm năng ứng dụng hiệu quả và ổn định trong xử lý nước thải dưới ánh sáng mặt trời, góp phần vào các giải pháp xử lý môi trường bền vững.

Từ khóa: MoS_2 hoa nano; Quang xúc tác; Methyl orange; Gốc oxy hoạt tính; Chiếu xạ mặt trời.